CORRECTION NOTICE

Nat. Neurosci. **16,** 210–218 (2013)

The organization of two new cortical interneuronal circuits

Xiaolong Jiang, Guangfu Wang, Alice J Lee, Ruth L Stornetta & J Julius Zhu

In the version of this supplementary file originally posted online, in Supplementary Figure 7a under SBC, the last 400 ms of trace 3 was a duplicate of trace 2; also, the corresponding legend referred to main-text Figure 7a,b instead of to Figure 8a,b. The errors have been corrected in this file as of 3 March 2013.

Supplementary Information for

The organization of two new cortical interneuronal circuits

Xiaolong Jiang[1,4], Guangfu Wang[1,4], Alice J. Lee[1,3], Ruth L. Stornetta[1] & J. Julius Zhu[1,2]

Departments of Pharmacology[1], Neuroscience[2], and Biology[3], School of Medicine and College of Arts and Sciences, University of Virginia, Charlottesville, VA 22908

Nature Neuroscience: doi:10.1038/nn.3305

Figure S1

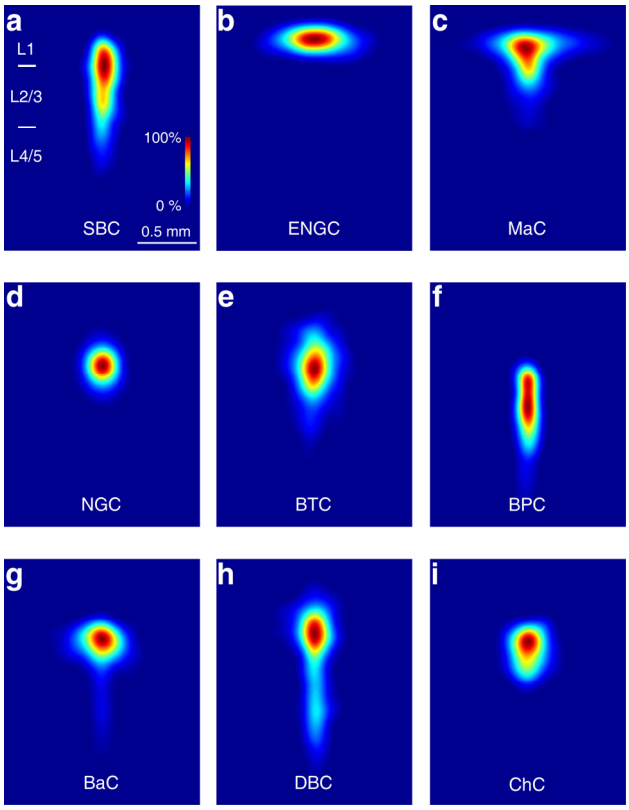

Fig. S1. Axonal length density maps of L1-3 interneurons.
(a-i) Axonal length density maps of L1 interneurons (SBC: *n*=17; ENGC: *n*=15) and L2/3 interneurons (MaC: *n*=15; NGC: *n*=28; BTCs: *n*=19; BPC: *n*=15; BaC: *n*=15; DBC: *n*=16; ChC: *n*=15).

Figure S2

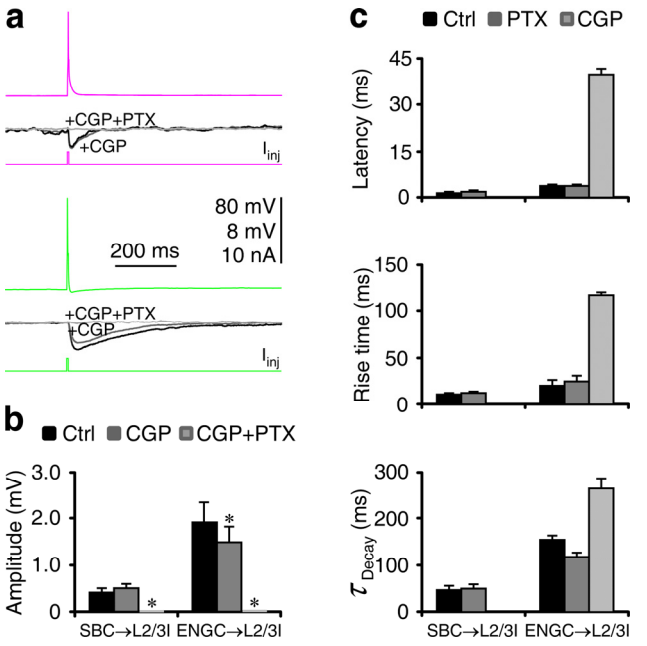

Fig. S2. SBCs and ENGCs form inhibitory circuits with different kinetics and GABA-R compositions.
(a) SBC- and ENGC-evoked uIPSPs in L2/3 interneurons from acute cortical slices before (black traces) and after (gray traces) bath application of 5 µM CGP35348, which blocks $GABA_B$ receptors, and 100 µM picrotoxin (PTX), which blocks $GABA_A$ receptors. Scale bars apply to all recording traces with 80 mV and 8 mV bars applied to traces with and without action potentials, respectively.
(b) The bar graphs show the amplitudes of SBC- and ENGC-evoked uIPSPs before and after bath application of CGP and PTX. Values for SBC-evoked uIPSPs (Ctrl: 0.41±0.10 mV; CGP: 0.48±0.09 mV; *n*=12, $\mathcal{Z}$=2.5; *p*=0.08; CGP+PTX: 0.00±0.00 mV; *n*=12, $\mathcal{Z}$=2.8; *p*<0.0005) and ENGC-evoked uIPSPs (Ctrl: 1.93±0.42 mV; CGP: 1.49±0.33 mV; *n*=8, $\mathcal{Z}$=2.5; *p*<0.05; CGP+PTX: 0.00±0.00 mV; *n*=8, $\mathcal{Z}$=2.6; *p*<0.0005). Asterisks indicate *p*<0.05 (Wilcoxon tests).
(c) The bar graphs show the latencies, rise times and decay time constants of PTX- and CGP35348-sensitive uIPSPs in L2/3 interneurons (SBC→MaC: *n*=1; SBC→NGCs: *n*=3; SBC→BTC: *n*=4; SBC→BPC: *n*=1; SBC→BaC: *n*=1; SBC→DBC: *n*=1; SBC→ChC: *n*=1; ENGC→MaC: *n*=1; ENGC→NGCs: *n*=3; ENGC→BTC: *n*=4). Values for the latencies (Ctrl: 1.5±0.2 ms; PTX: 1.8±0.3 ms; *n*=12 for SBC-evoked uIPSPs; Ctrl: 3.9±0.5 ms; PTX: 3.8±0.4 ms; CGP: 39.5±1.6 ms; *n*=8 for ENGC-evoked uIPSPs), rise times (Ctrl: 11.2±1.4 ms; PTX: 12.4±2.0 ms; *n*=12 for SBC-evoked uIPSPs; Ctrl: 20.3±2.5 ms; PTX: 25.1±5.1 ms; CGP: 116.3±2.6 ms; *n*=8 for ENGC-evoked uIPSPs), and decay time constants (Ctrl: 41.3±5.5 ms; PTX: 40.3±3.7 ms; *n*=12 for SBC-evoked uIPSPs; Ctrl: 154.3±6.1 ms; PTX: 115.9±9.1 ms; CGP: 262.2±22.1 ms; *n*=8 for ENGC-evoked uIPSPs). Note that CGP- and PTX-sensitive uIPSPs were calculated by digitally subtracting the evoked responses after including additional CGP and PTX in the bath solution, respectively.

Figure S3

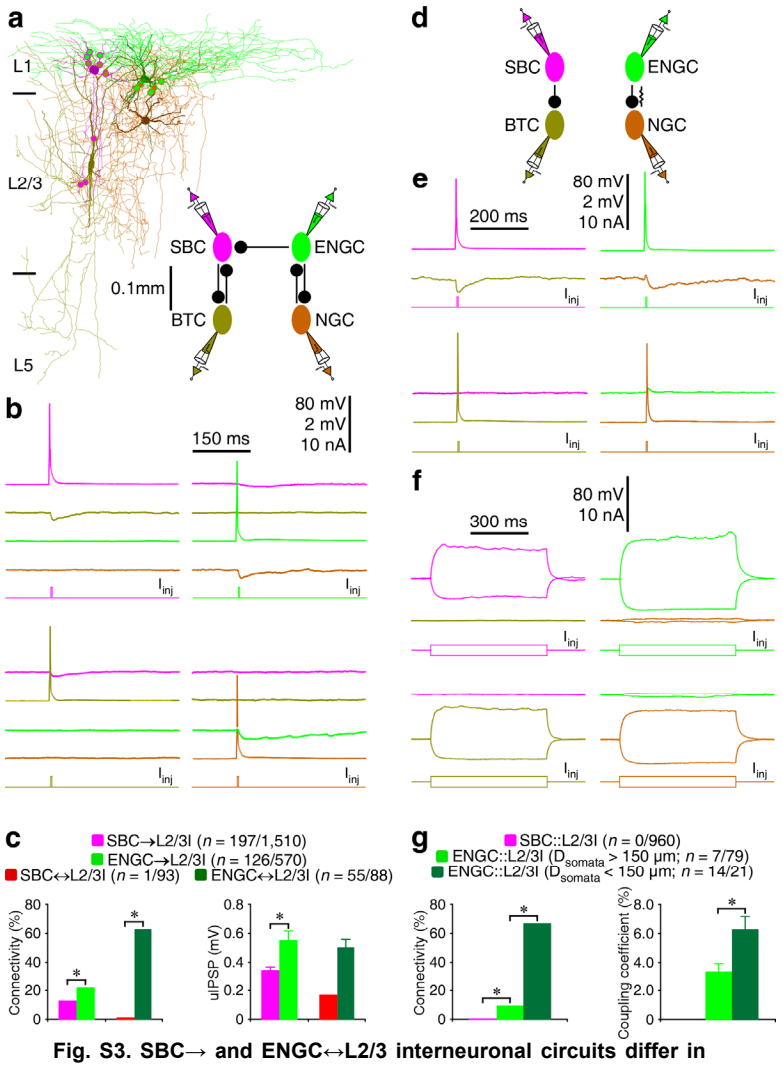

Fig. S3. SBC→ and ENGC↔L2/3 interneuronal circuits differ in synaptic connectivity.

(a) Reconstruction of L1 SBC (pink), L1 ENGC (green), L2/3 BTC (yellow) and L2/3 NGC (brown) recorded simultaneously from an acute cortical slice. The double colored dots indicate the putative synaptic contacts. The schematic drawing shows symbolically their synaptic connections.
(b) Single action potentials elicited in presynaptic L1-3 interneurons evoked uIPSPs in postsynaptic L1-3 interneurons.
(c) The bar graphs show the connectivity and strength of synapses formed between L1-3 interneurons located within the same column. Values for the connectivity (SBC→L2/3I: 13.0%, n=197 of 1510 tested connections; ENGC→L2/3I: 22.1%, n=126 of 570 tested connections; χ^2=25.9; p<0.0005; SBC↔L2/3I: 1.1%, n=1 of 93 tested SBC→L2/3I pairs; ENGC↔L2/3I: 62.5%, n=55 of 88 tested ENGC→L2/3I pairs; χ^2=79.8; p<0.0005; Chi-squared tests), and strength (SBC→L2/3I: 0.34±0.03 mV, n=128; ENGC→L2/3I: 0.54±0.07 mV, n=80; U=3,499; p<0.005; Mann-Whitney Rank Sum test; L2/3I→SBC: 0.17 mV, n=1 SBC↔L2/3I pair; L2/3I→ENGC: 0.50±0.06 mV, n=53 ENGC↔L2/3I pairs).
(d) The schematic drawing shows symbolically inhibitory connections between SBC and BTC, and inhibitory and electric connections between ENGC and NGC recorded from an acute cortical slice.
(e) The recording traces show that single action potentials elicited in presynaptic SBC evoked uIPSPs in postsynaptic BTC, single action potentials elicited in presynaptic ENGC evoked spikelets and uIPSPs in postsynaptic NGC, and single action potentials elicited in NGC evoked spikelets in postsynaptic ENGC.
(f) The recording traces show that the depolarizing and hyperpolarizing current injections in SBC and BTC had no effect on the membrane potentials of BTC and SBC, respectively, and the current injections in ENGC and NGC induced small membrane depolarization and hyperpolarization in NGC and ENGC, respectively. Scale bars in **b**, **e** and **f** apply to all recording traces with 80 mV and 2 mV bars applied to traces with and without action potentials, respectively.
(g) The bar graphs show the connectivity and coupling coefficient of electric synapses formed between L1 and L2/3 interneurons. Values for the electric synapse connectivity (SBC::L2/3I: 0.0%, n=0 of 960 tested pairs; ENGC::L2/3I: 9.1%, n=7 of 79 tested pairs with intersomatic distance >150 µm; χ^2=85.6; p<0.0005; ENGC::L2/3I: 66.7%, n=14 of 21 tested pairs with intersomatic distance <150 µm; χ^2=649.3; p<0.0005; Chi-squared tests), and coupling coefficient (ENGC::L2/3I: 3.30±0.59%, n=7 pairs with intersomatic distance >150 µm; ENGC::L2/3I: 6.22±0.91%, n=14 pairs with intersomatic distance <150 µm; U=77.0; p<0.05; Mann-Whitney Rank Sum test). Asterisks in **c** and **g** indicate p<0.05 (Chi-squared or Mann-Whitney Rank Sum tests).

Figure S4

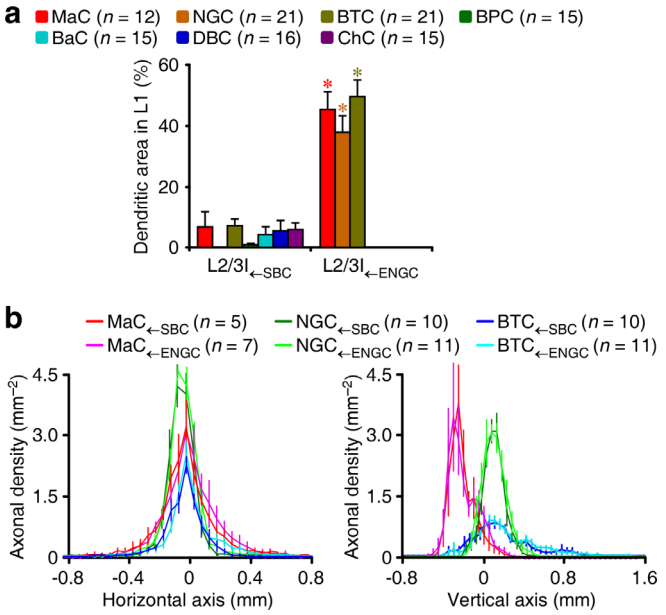

Fig. S4. L2/3 interneurons in SBC→ and ENGC↔L2/3 interneuronal circuits differ in dendritic anatomy.
(a) L1 fractions of dendritic arborization of L2/3 interneurons targeted by SBCs and ENGCs (MaC$_{\leftarrow SBC}$: 6.5±5.1%, n=5; MaC$_{\leftarrow ENGC}$: 45.5±5.6%, n=7; U=0.0; p<0.005; NGC$_{\leftarrow SBC}$: 0.0±0.0%, n=10; NGC$_{\leftarrow ENGC}$: 37.8±5.8%, n=11; U=0.0; p<0.0001; BTC$_{\leftarrow SBC}$: 7.0±2.2%, n=10; BTC$_{\leftarrow ENGC}$: 49.7±5.2%, n=11; U=0.0; p<0.0001; BPC: 0.9±0.3%, n=15; BaC: 4.3±2.1%, n=15; DBC: 5.4±3.2%, n=16; ChC: 6.0±1.9%, n=15). Asterisks indicate p<0.05 (Mann-Whitney Rank Sum tests).
(b) Axonal length density plots targeted by SBCs and ENGCs (MaC$_{\leftarrow SBC}$: n=5; MaC$_{\leftarrow ENGC}$: n=7; F=0.4; p>0.05; NGC$_{\leftarrow SBC}$: n=10; NGC$_{\leftarrow ENGC}$: n=11; F=1.8; p>0.05; BTC$_{\leftarrow SBC}$: n=10; BTC$_{\leftarrow ENGC}$: n=11; F=2.7; p>0.05; ANOVA tests). Mann-Whitney Rank Sum tests indicate that the soma of MaCs, NGCs and BTCs targeted by SBCs were located deeper in L2/3 than that of MaCs, NGCs and BTCs targeted by ENGCs (MaC$_{\leftarrow SBC}$: 161.8±19.9 µm; n=5; MaC$_{\leftarrow ENGC}$: 76.0±8.3 µm; n=7; U=0.0; p<0.05; NGC$_{\leftarrow SBC}$: 166.7±17.8 µm; n=10; NGC$_{\leftarrow ENGC}$: 44.2±6.0 µm; n=11; U=0.0; p<0.01; BTC$_{\leftarrow SBC}$: 161.3±22.4 µm; n=10; BTC$_{\leftarrow ENGC}$: 66.3±5.0 µm; n=11; U=0.0; p<0.01).

Figure S5

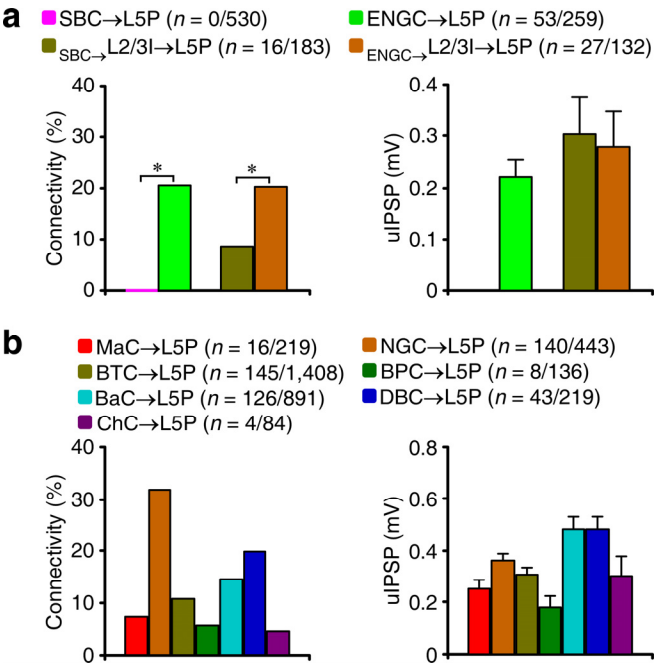

Fig. S5. SBC→ and ENGC↔L2/3I interneuronal circuits differentially innervate L5 pyramidal neurons.
(a) The bar graphs show the connectivity and strength of synapses formed between SBCs, ENGCs, L2/3 interneurons postsynaptic to SBCs, or L2/3 interneurons postsynaptic to ENGCs, and L5 pyramidal neurons within the same column. Values for the connectivity (SBC→L5P: 0.0%, n=0 of 530 tested connections; ENGC→L5P: 20.4%, n=53 of 259 tested connections; χ^2=116.3; p<0.005; $_{SBC\rightarrow}$L2/3I→L5P: 8.7%, n=16 of 183 tested connections; $_{ENGC\leftrightarrow}$L2/3I→L5P: 20.5%, n=27 of 132 tested connections; χ^2=8.8; p<0.005; Chi-squared tests) and strength (ENGC→L5P: 0.22±0.03 mV, n=19; $_{SBC\rightarrow}$L2/3I→L5P: 0.30±0.07 mV, n=15; $_{ENGC\leftrightarrow}$L2/3I→L5P: 0.28±0.07 mV, n=15; U=115.0; p=0.92; Mann-Whitney Rank Sum test). Note that ENGCs, but not L2/3 interneurons postsynaptic to ENGCs, form synapses on L5 pyramidal neurons located in both the same and neighboring columns (ENGC→L5P$_{\text{same column}}$: 20.4%, n=53/259; ENGC→L5P$_{\text{neighboring column}}$: 5.2%, n=6/116; χ^2=14.1; p<0.005; $_{ENGC\leftrightarrow}$MaC→L5P$_{\text{same column}}$: 7.1%, n=1/14; $_{ENGC\leftrightarrow}$MaC→L5P$_{\text{neighboring column}}$: 0.0%, n=0/14; χ^2=1.0; p=0.301; $_{ENGC\leftrightarrow}$NGC→L5P$_{\text{same column}}$: 33.3%, n=17/51; $_{ENGC\leftrightarrow}$NGC→L5P$_{\text{neighboring column}}$: 0.0%, n=0/23; χ^2=10.0; p<0.005; $_{ENGC\leftrightarrow}$BTC→L5P$_{\text{same column}}$: 15.8%, n=9/57; $_{ENGC\leftrightarrow}$BTC→L5P$_{\text{neighboring column}}$: 0.0%, n=0/23; χ^2=4.1;

p<0.05; Chi-squared tests). Asterisks indicate p<0.05 (Chi-squared tests).
(b) The bar graphs show the connectivity and strength of synapses formed between L2/3 interneurons and L5 pyramidal neurons within the same column. Values for the strength (MaC→L5P: 0.24±0.03 mV, n=11; NGC→L5P: 0.35±0.03 mV, n=88; BTC→L5P: 0.30±0.03 mV, n=89; BPC→L5P: 0.17±0.04 mV, n=8; BaC→L5P: 0.47±0.05 mV, n=67; DBC→L5P: 0.47±0.05 mV, n=41; ChC→L5P: 0.29±0.07 mV, n=4; F=3.8; p<0.005; ANOVA test). Note that L2/3 interneurons form synapses on L5 pyramidal neurons located in the same columns, but not those in neighboring columns (MaC→$L5P_{same\ column}$: 7.3%, n=16/219; MaC→$L5P_{neighboring\ column}$: 0.0%, n=0/74; χ^2=5.7; p<0.05; NGC→$L5P_{same\ column}$: 31.6%, n=140/443; NGC→$L5P_{neighboring\ column}$: 0.0%, n=0/37; χ^2=16.5; p<0.005; BTC→$L5P_{same\ column}$: 10.3%, n=145/1,408; BTC→$L5P_{neighboring\ column}$: 0.0%, n=0/106; χ^2=11.8; p<0.005; BPC→$L5P_{same\ column}$: 4.6%, n=8/136; BPC→$L5P_{neighboring\ column}$: 0.0%, n=0/81; χ^2=4.9; p<0.05; BaC→$L5P_{same\ column}$: 14.1%, n=126/891; BaC→$L5P_{neighboring\ column}$: 0.0%, n=0/51; χ^2=8.3; p<0.05; DBC→$L5P_{same\ column}$: 19.6%, n=43/219; DBC→$L5P_{neighboring\ column}$: 0.0%, n=0/43; χ^2=19.1; p<0.005; ChC→$L5P_{same\ column}$: 4.8%, n=4/84; p<0.005; ChC→$L5P_{neighboring\ column}$: 0.0%, n=0/76; χ^2=3.7; p<0.05; Chi-squared tests).

Figure S6

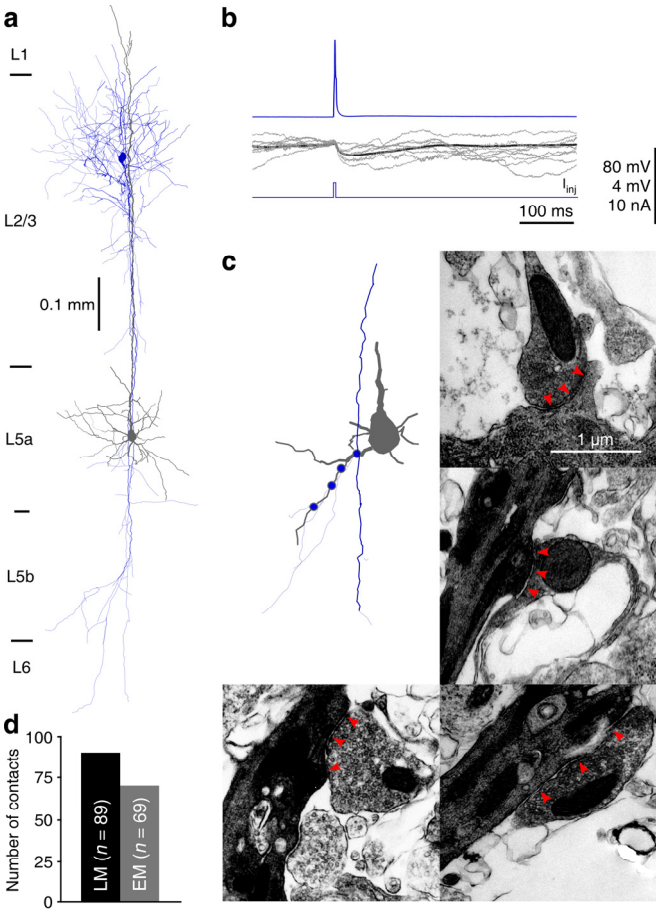

Fig. S6. EM confirms the majority of LM-identified synaptic boutons.
(a) Reconstruction of L2/3 DBC (blue) and L5 pyramidal neuron (grey) recorded simultaneously from an acute cortical slice. The double colored dots indicate the putative synaptic contacts identified by LM.
(b) Single action potentials elicited in presynaptic DBC evoked uIPSPs in postsynaptic L5 pyramidal neuron. 80 mV and 4 mV bars apply to traces with and without action potentials, respectively. Note the average uIPSP trace (black), as well as superimposed individual uIPSP traces (gray).
(c) Four light microscopy (LM)-identified synaptic boutons were confirmed with electron microscopy (EM). Arrow heads in EM images indicate synaptic junctions established by the axon of DBC.
(d) The numbers of LM- and EM-identified synapses.

Figure S7

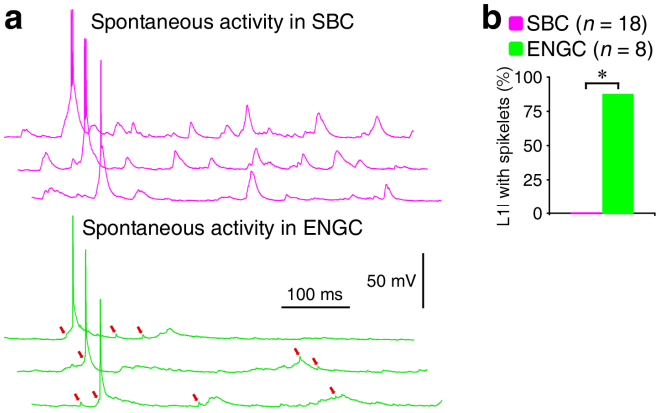

Fig. S7. Spikelet-like events are prevalent in ENGCs recorded *in vivo*.
(a) Spontaneous recording traces of the SBC and ENGC in figure 8a-b in expanded scales. Red arrows indicate the spikelets characteristic of electric synapses. Note the spikelets absent in SBC, but prevalent in ENGC. Scale bars apply to all recording traces.
(b) Percentages of L1 interneurons displayed the spikelets (SBCs: 0%, n=0/18; ENGCs: 87.5%, n=7/8; χ^2=21.6). Asterisk indicates p<0.05 (Chi-squared test).

Figure S8

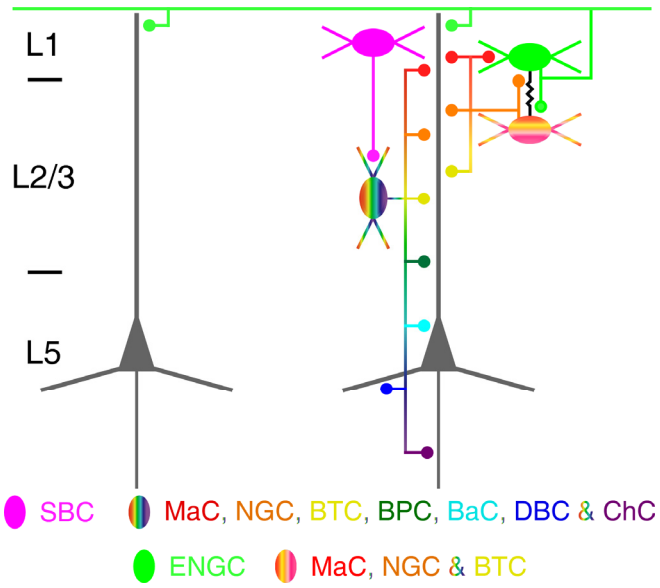

Fig. S8. Schematic drawing shows key features of SBC→ and ENGC↔L2/3I→L5 pyramidal neuronal circuits.
See the main text for the detailed architecture of the two cortical interneuronal circuits.

Table S1

Synaptic connectivity between L1 and L2/3 interneurons

Cell connection pattern	L2/3Is in same columns (Connected/tested and %)		L2/3Is in neighboring columns (Connected/tested and %)		χ^2 and *P* value (Chi-squared)	
SBC→MaC	6/124	4.8%	0/79	0.0%	3.9	0.047
SBC→NGC	18/250	7.3%	0/69	0.0%	5.3	0.022
SBC→BTC	68/466	14.6%	0/76	0.0%	12.7	0.000
SBC→BPC	34/122	27.9%	0/19	0.0%	7.0	0.008
SBC→BaC	29/305	9.5%	0/64	0.0%	6.6	0.012
SBC→DBC	7/82	8.5%	0/43	0.0%	3.9	0.048
SBC→ChC	13/75	17.3%	0/22	0.0%	4.4	0.036
ENGC→MaC	11/60	18.3%	1/18	5.5%	1.7	0.188
ENGC→NGC	46/108	42.6%	3/22	13.2%	6.5	0.011
ENGC→BTC	62/192	32.3%	4/27	14.8%	3.4	0.064
ENGC→BPC	0/34	0.0%	0/7	0.0%	--	
ENGC→BaC	0/119	0.0%	0/23	0.0%	--	
ENGC→DBC	0/31	0.0%	0/11	0.0%	--	
ENGC→ChC	0/17	0.0%	0/4	0.0%	--	

Cell connection pattern	SBCs (Connected/tested and %)		ENGCs (Connected/tested and %)		χ^2 and *P* value (Chi-squared)	
MaC→L1I	43/109	39.4%	27/49	55.1%	3.4	0.067
NGC→L1I	41/152	27.0%	41/79	51.9%	14.1	0.000
BTC→L1I	9/282	3.2%	19/126	15.1%	19.3	0.003
BPC→L1I	0/58	0.0%	0/18	0.0%	--	
BaC→L1I	1/174	0.6%	4/72	5.6%	6.3	0.012
DBC→L1I	0/60	0.0%	0/25	0.0%	--	
ChC→L1I	0/36	0.0%	0/18	0.0%	--	
MaC↔L1I	0/43	0.0%	9/27	33.3%	16.4	0.000
NGC↔L1I	0/41	0.0%	30/41	73.2%	47.3	0.000
BTC↔L1I	1/9	11.1%	15/19	79.9%	11.5	0.000

Note that SBCs rarely form mutual inhibitory connections with L2/3 MaCs, NGCs and BTCs, even though many of which, presumably interconnected with ENGCs, inhibit SBCs.

Table S2

Correlation of physiology-, LM- and EM-identified inhibitory connections on L5 pyramidal neurons

Cell connection pattern	Connected pairs (LM/physiology)	No. of boutons in LM-identified pairs	Unconnected pairs (LM/physiology)	χ^2 and *P* value* (Chi-squared)	
ENGC→L5P	6/7	4.5±0.7 (*n*=6)	11/11	1.7	0.729
MaC→L5P	10/11	5.4±0.4 (*n*=10)	14/14	1.3	0.774
NGC→L5P	17/17	3.7±0.3 (*n*=17)	29/30	0.6	0.831
BTC→L5P	27/28	5.7±0.6 (*n*=27)	71/71	2.6	0.874
BPC→L5P	8/8	4.3±0.4 (*n*=8)	14/14	--	1.000
BaC→L5P	28/31	3.8±0.3 (*n*=26)	42/43	1.9	0.501
DBC→L5P	26/27	4.1±0.3 (*n*=26)	24/24	0.9	0.843
ChC→L5P	4/4	3.8±0.6 (*n*=4)	10/10	--	1.000

Cell connection pattern	No. of cell pairs	No. of LM-identified synapses	No. of EM-identified synapses	Confirmation rate (%)
MaC→L5P	1	6	5	83.3%
NGC→L5P	6	38	26	68.4%
BTC→L5P	3	18	15	83.3%
BPC→L5P	1	4	3	75.0%
BaC→L5P	4	19	16	84.2%
DBC→L5P	1	4	4	100.0%
Total	15	89	69	77.5%

*Note the Chi-squared tests show no difference between physiologically and light microscopically identified synaptic connections formed between various types of L1-3 interneurons and L5 pyramidal neurons.

Table S3

Synaptic connectivity and strength between L1 and L2/3 interneurons in different cortical areas

Presynaptic cell type	L2/3Is in sensory cortex (Connected/tested and %)		L2/3Is in motor cortex (Connected/tested and %)		χ^2 and *P* value (Chi-squared)	
SBC	110/801	13.7%	52/469	11.1%	1.9	0.171
ENGC	40/186	21.5%	16/77	20.8%	0.0	0.895

Presynaptic cell type	L2/3Is in sensory cortex (mV)	L2/3Is in motor cortex (mV)	*U and P* value (M-W Rank Sum)	
SBC	0.34±0.04 (*n*=110)	0.35±0.05 (*n*=52)	858	0.115
ENGC	0.68±0.10 (*n*=40)	0.60±0.14 (*n*=16)	370	0.080

Table S4

Synaptic connectivity and strength between L1-3Is and L5 pyramidal neurons in different cortical areas

Presynaptic cell type	L5Ps in sensory cortex (Connected/tested and %)		L5Ps in motor cortex (Connected/tested and %)		χ^2 and *P* value (Chi-squared)	
MaC	7/112	6.3%	5/83	6.0%	0.0	0.791
NGC	88/279	31.5%	30/99	30.3%	0.1	0.819
BTC	82/831	9.9%	30/319	9.4%	0.1	0.812
BPC	3/66	4.5%	1/26	3.9%	0.0	0.882
BaC	72/507	14.2%	31/238	13.0%	0.2	0.662
DBC	23/127	18.1%	13/63	20.6%	0.2	0.676
ChC	2/44	4.5%	1/19	5.3%	0.0	0.902
ENGC	13/72	18.1%	9/49	18.3%	0.0	0.965

Presynaptic cell type	L5Ps in sensory cortex (mV)	L5Ps in motor cortex (mV)	*U and P* value (M-W Rank Sum)	
MaC	0.25±0.06 (*n*=7)	0.22±0.04 (*n*=5)	14	0.931
NGC	0.42±0.06 (*n*=88)	0.39±0.06 (*n*=30)	1,048	0.268
BTC	0.30±0.06 (*n*=82)	0.29±0.03 (*n*=30)	1,111	0.492
BPC	0.18±0.10 (*n*=3)	0.14 (*n*=1)	--	
BaC	0.51±0.10 (*n*=72)	0.49±0.12 (*n*=31)	975	0.484
DBC	0.59±0.11 (*n*=23)	0.47±0.07 (*n*=13)	135	0.553
ChC	0.24 (*n*=2)	0.26 (*n*=1)	--	
ENGC	0.25±0.04 (*n*=13)	0.26±0.06 (*n*=9)	54	0.690

Movie S1. 3D reconstruction reveals distinguished axonal anatomy of SBCs and ENGCs.
This movie shows the 3D structure of L1 SBC (pink) and L1 ENGC (green) recorded from an acute cortical slice.

Movie S2. 3D reconstruction reveals distinguished axonal anatomy of L2/3 interneurons.
This movie shows the 3D structure of L2/3 MaC (red), NGC (orange), BTC (yellow), BPC (dark green), BaC (cyan), DBC (blue) and ChC (purple) recorded from acute cortical slices.